Electronic Supplementary Information

H-bonding-mediated binding and charge reorganization of proteins onto gold nanoparticles

Brahmaiah Meesaragandla,[a,b] Isabel Garcia,[c] Doreen Biedenweg,[b] Jhoan Toro-Mendoza,[c] Ivan Coluzza,[c,d] Luis M. Liz-Marzán,[c,d] and Mihaela Delcea[a,b,e*]

[a]*Institute of Biochemistry, University of Greifswald, Felix-Hausdorff-Straße 4, 17489 Greifswald, Germany;*
[b]*ZIK HIKE- Zentrum für Innovationskompetenz „Humorale Immunreaktionen bei kardiovaskulären Erkrankungen", Fleischmannstraße 42, 17489 Greifswald, Germany;*
[c3]*CIC biomaGUNE and CIBER de Bioingeniería, Biomateriales y Nanomedicina (CIBER-BBN), Paseo de Miramón 182, 20014 Donostia-San Sebastián, Spain*
[d]*Ikerbasque, Basque Foundation for Science, 48013 Bilbao, Spain*
[e]*DZHK (Deutsches Zentrum für Herz-Kreislauf-Forschung), partner site Greifswald, Germany*

Corresponding author: Prof. Dr. Mihaela Delcea: delceam@uni-greifswald.de

Table S1. Hydrodynamic diameter determined by dynamic light scattering and ζ-potential of functionalized AuNPs.

AuNP	Size (nm)	Zeta potential (mV)
Citrate-AuNPs	19.31 ± 0.1	-13.2 ± 0.9
PEG-OMe-AuNPs	46.61 ± 0.4	-1.8 ± 0.1
PEG-COOH AuNPs	44.06 ± 0.3	-8.3 ± 0.3
PEG-NH_2-AuNPs	43.95 ± 0.2	+5.3 ± 0.4
Glycan-AuNPs	34.15 ± 0.3	-2.9 ± 0.3

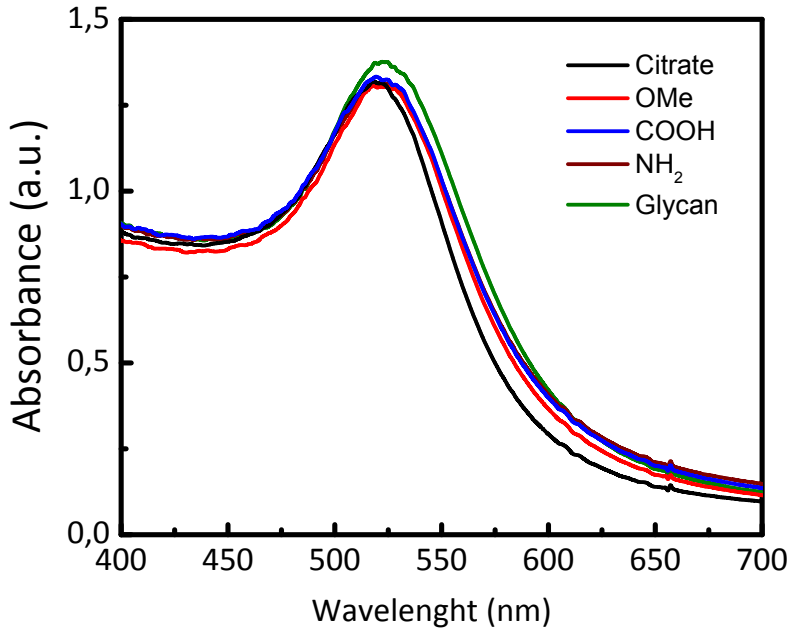

Figure S1: UV-Vis spectra of AuNPs before (citrate-, black) and after surface modification with PEG-OMe (red), PEG-COOH (blue), PEG-NH_2 (brown) and lactose (green) ligands, respectively.

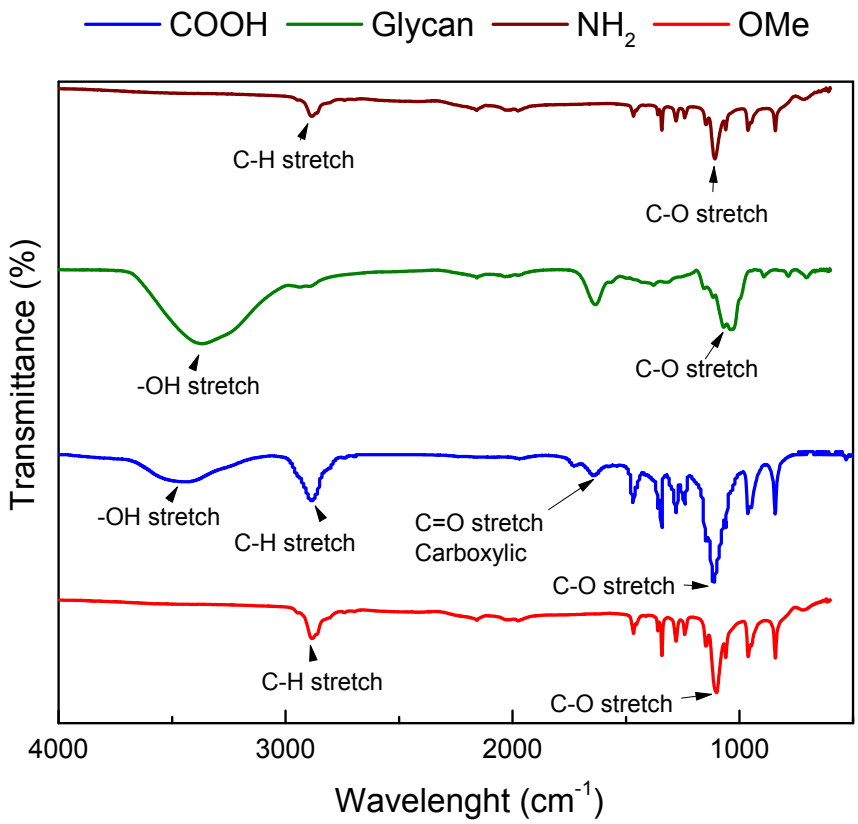

Figure S2. FTIR spectra of AuNPs modified with PEG-OMe (red) PEG-COOH (blue), glycan (green) and PEG-NH_2 (brown).

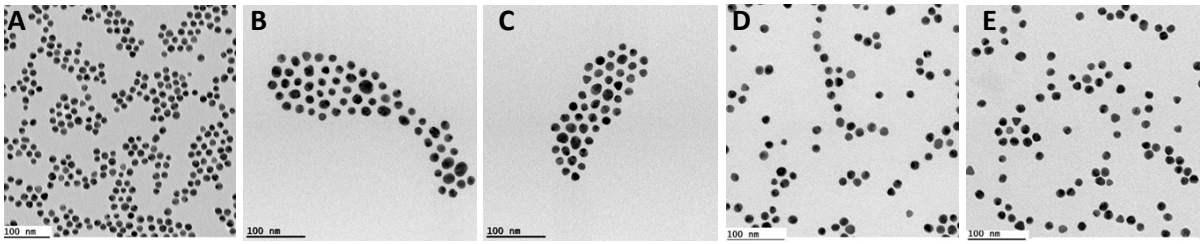

Figure S3. TEM images of AuNPs prior and after surface modification with (A) citrate (B) PEG-OMe, (C) glycan, (D) PEG-COOH, and (E) PEG-NH_2.

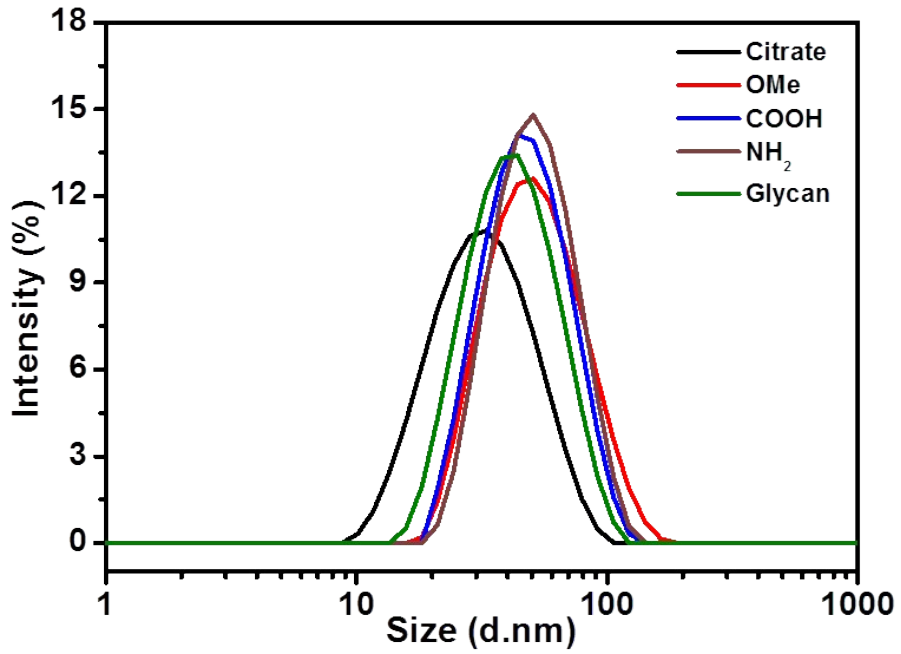

Figure S4. Size (d.nm) of AuNPs with different functionalities: citrate (black); PEG-OMe (red); PEG-COOH (blue); PEG-NH_2 (brown) and glycan (green) in water.

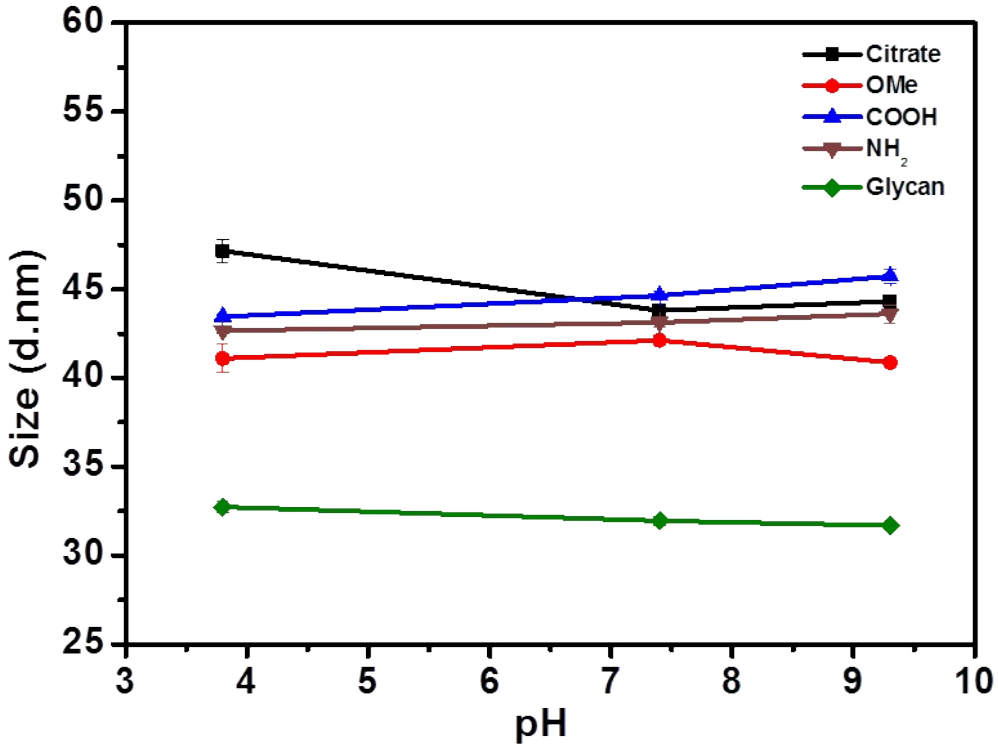

Figure S5. Size of AuNP-HSA bioconjugates formed from surface modified AuNPs, at pH 3.8, 7.4 and 9.3. (The lines between data are guides to the eye). (HSA concentration =2.4×10^{-6} M)

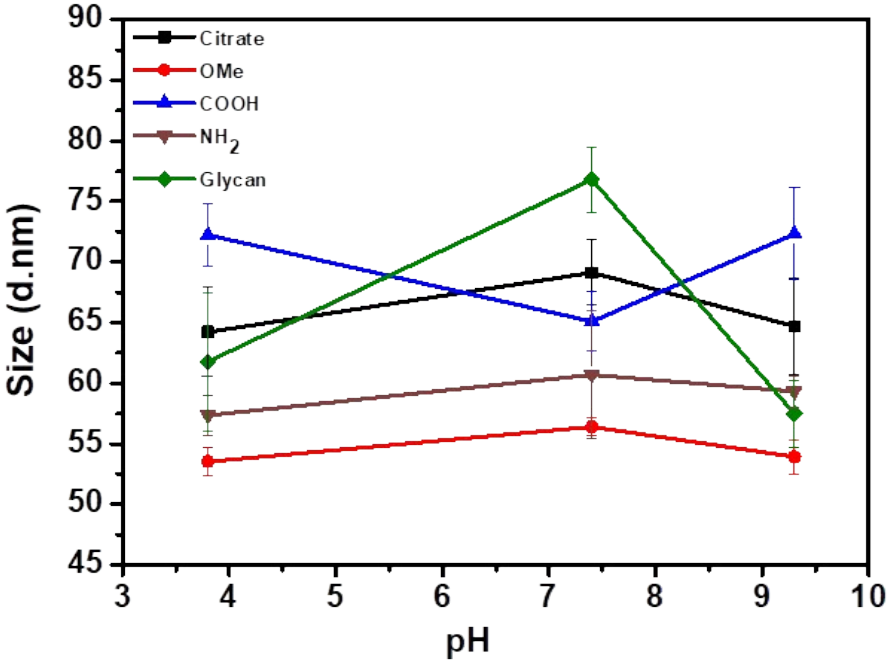

Figure S6. Size of AuNP-HSA bioconjugates formed from surface-modified AuNPs, at pH 3.8; 7.4 and 9.3. (HSA concentration = 7.5×10^{-3} M).

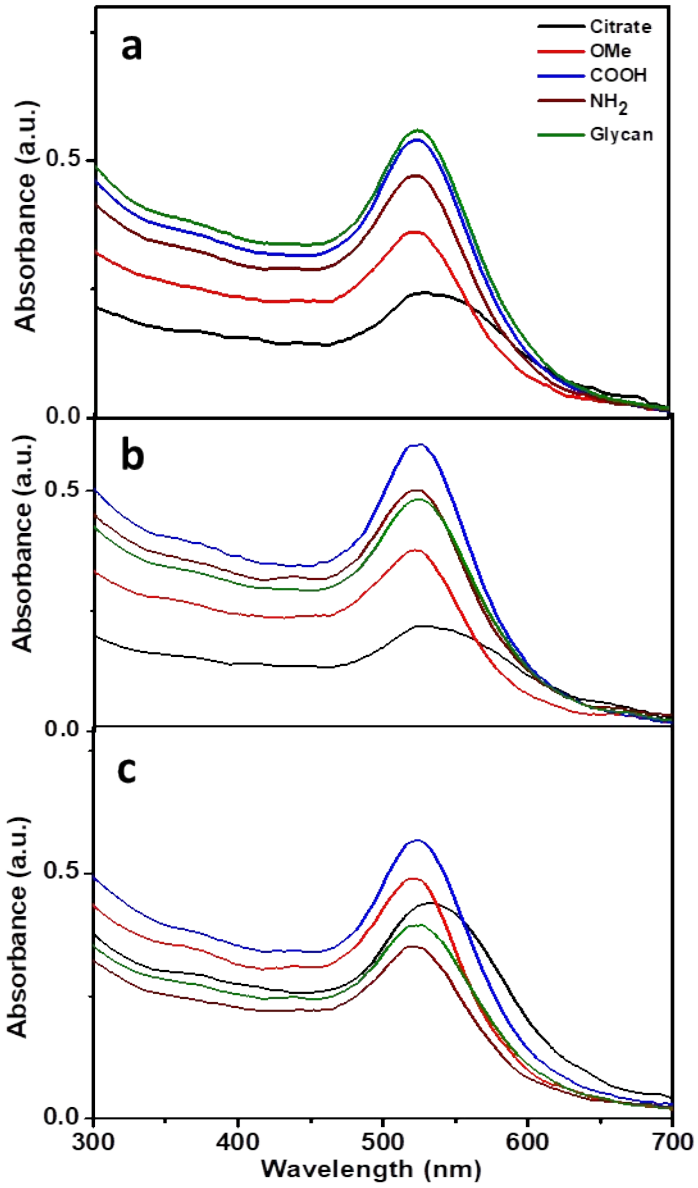

Figure S7. UV-Vis absorption spectra of AuNP-HSA bioconjugates with different surface modified AuNPs at pH 3.8 (a), pH 7.4 (b) and pH 9.3 (c).

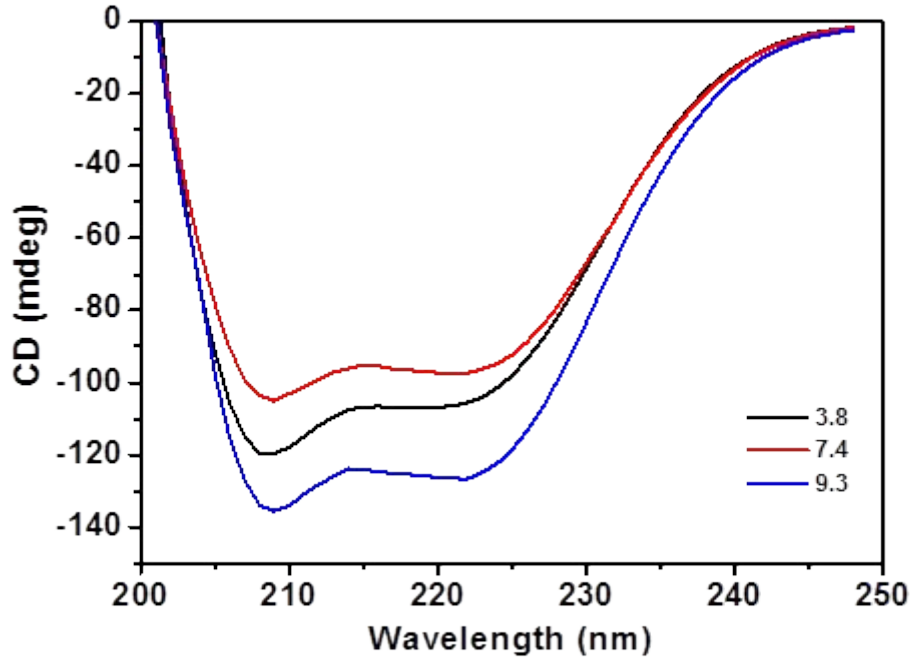

Figure S8. Far-UV CD spectra of HSA at pH 3.8 (black), pH 7.4 (red), and pH 9.3 (blue).

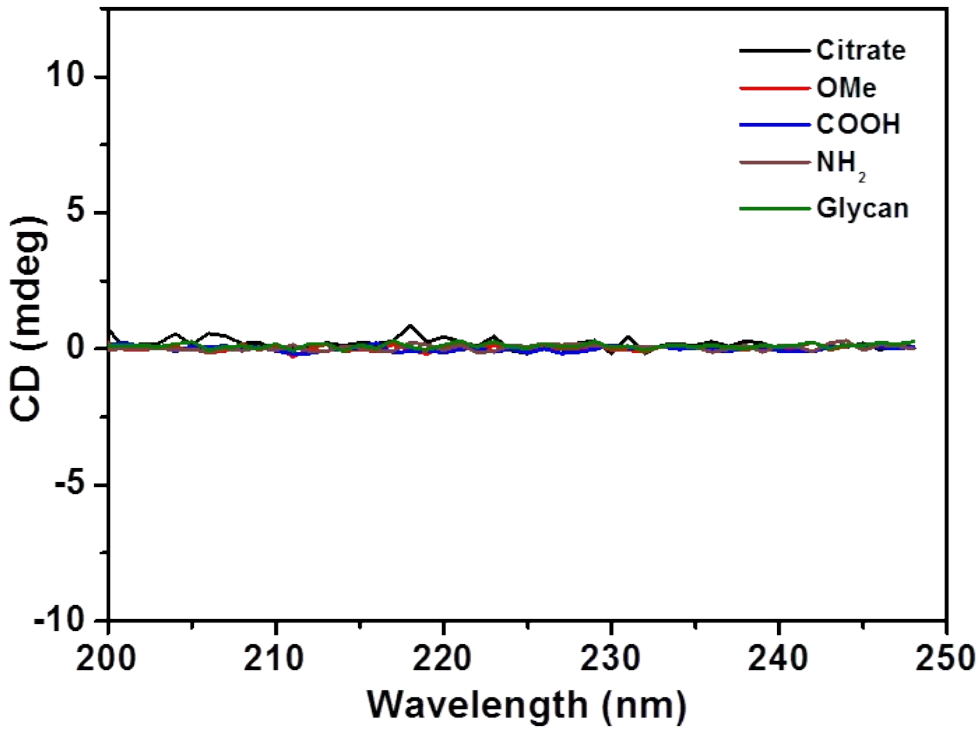

Figure S9. Far-UV CD spectra of AuNPs with different surface modifications, indicating no CD signal.

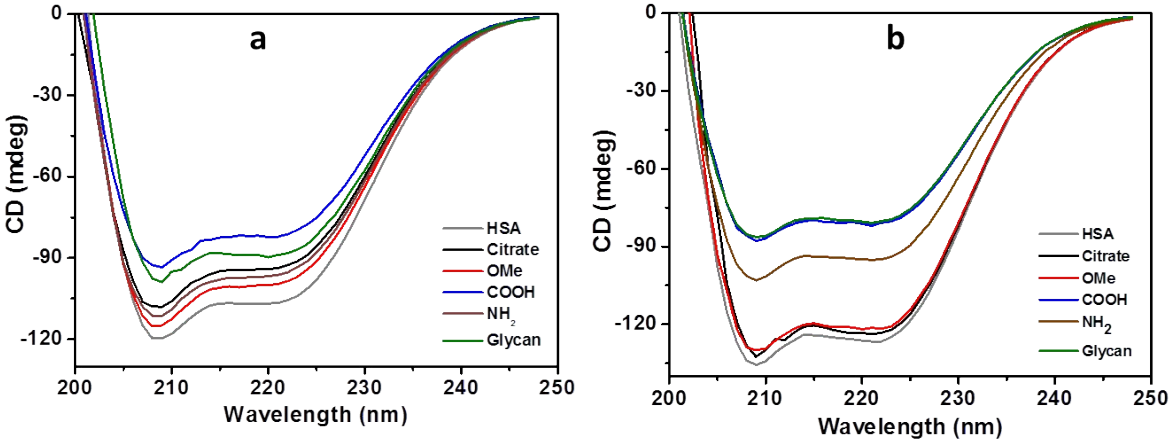

Figure S10. CD spectra of native HSA (2.4×10^{-6} M) and Au-HSA bioconjugates with different surface modified AuNPs, at pH values of 3.8 (a), and 9.3 (b).

Table S2. Percentages of secondary structures of HSA and the same upon interaction with different surface-modified AuNPs at various pHs.

pH		Secondary structures				
		Helix (%)	Antiparallel (%)	Parallel (%)	Turns (%)	Others(%)
3.8	HSA	42.4	10.5	3.2	13.6	30.3
	Citrate	35.2	13.5	4.0	14.2	33.1
	P-OMe	38.3	11.5	4.0	13.6	32.5
	P-NH_2	37.1	9.8	4.4	14.1	34.5
	P-COOH	31.3	14.2	5.5	12.5	36.5
	Glycan	33.8	16.7	3.8	14.5	31.2
7.8	HSA	48.8	9.5	1.8	12.6	27.3
	Citrate	38.4	11.3	4.1	13.9	32.4
	P-OMe	46.8	8.2	2.6	12.9	29.5
	P-NH_2	35.2	13.5	5.1	14.2	31.9
	P-COOH	46.7	6.8	3.2	12.7	30.6
	Glycan	49.5	8.2	2.8	12.2	27.2
9.3	HSA	47.8	13.0	1.0	12.2	26.0
	Citrate	51.3	18.3	0.0	13.2	17.2
	P-OMe	49.9	8.2	2.3	12.9	26.7
	P-NH_2	34.9	11.9	6.7	12.3	34.1
	P-COOH	30.3	17.7	7.4	11.2	33.4
	Glycan	27.5	15.8	7.7	14.1	34.9

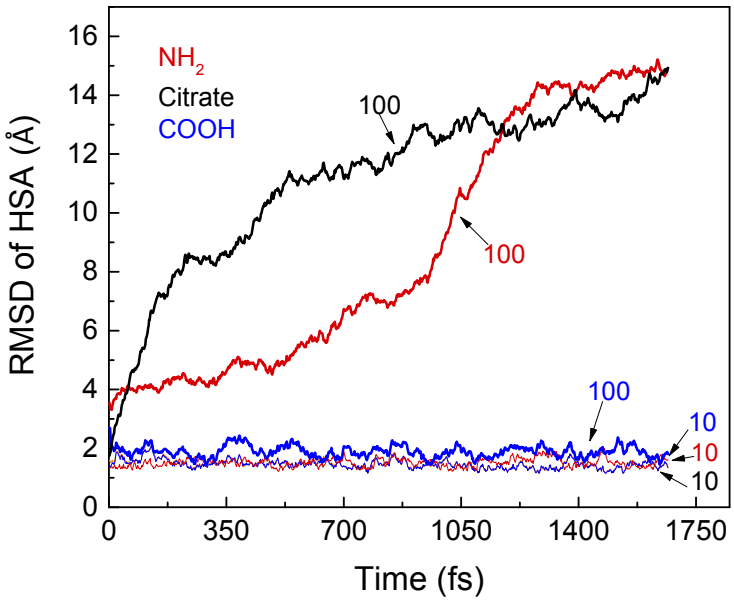

Figure S11. Root mean square displacements representing the changes of HSA in presence of three different coated NPs, estimated from MD simulations at two different magnitudes of the attractive forces F (numbers highlighted therein).